ACS Catalysis

Research Article

pubs.acs.org/acscatalysis

An Efficient Reusable Mesoporous Solid-Based Pd Catalyst for Selective C2 Arylation of Indoles in Water

Linlin Duan,[†] Rao Fu,[†] Bingsen Zhang,*[,‡] Wen Shi,[‡] Shangjun Chen,[†] and Ying Wan*[,†]

[†]Key Laboratory of Resource Chemistry of Ministry of Education, Shanghai Key Laboratory of Rare Earth Functional Materials, and Department of Chemistry, Shanghai Normal University, Shanghai 200234, People's Republic of China

[‡]Shenyang National Laboratory for Materials Science, Institute of Metal Research, Chinese Academy of Sciences, Shenyang 110016, People's Republic of China

Supporting Information

ABSTRACT: The completely C2-selective arylation of *N*-methylindole was achieved by using a reusable solid Pd catalyst and water as a solvent without any other ligands or additives or exclusion of air. The catalysts possess well-dispersed Pd nanoparticles (~1.5 nm), N-containing functional groups (~11 wt %), and uniform mesopores (~5 nm). The turnover frequency (TOF) is calculated to be 82 h^{-1}.Arylations of both *N*-H indoles and N-protected indoles with diaryliodonium salts were achieved to give the desired products in high to excellent isolated yields in water. Mercapto-functionalized silica as a selective trapping agent, together with hot filtration, confirms the undetected leaching of Pd. The catalyst samples can be reused at least eight times without any additional activation treatment. The catalytic performance of the Pd catalyst is also compared with the performance of other mesoporous Pd catalysts on silica, carbon, and resins. The catalytic activity and stability of the present catalyst may be related to the well-dispersed Pd nanoparticles, the electron-rich environment stabilized by the N-containing functional groups, and the large, uniform mesopores.

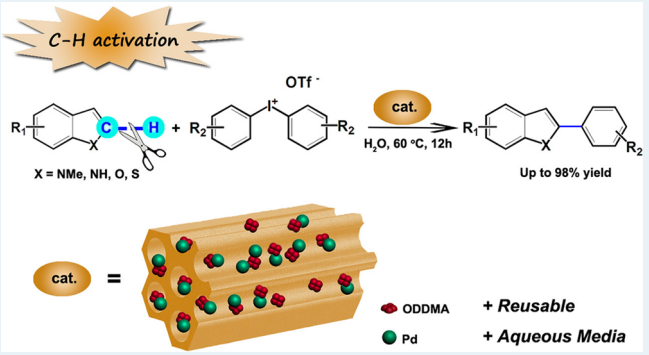

KEYWORDS: *C2 arylation, Pd cluster, hybrid mesoporous polymer, water-mediated, reusability*

1. INTRODUCTION

The direct functionalization of the C−H bond is a fundamentally important subject in organic synthesis in both academic and industrial processes. During the past decade, we have witnessed the development of a wide range of metal-catalyzed reactions that allow direct C−H bond transformation.[1] The majority of the work has been performed in organic solvents and often under relatively harsh conditions.[2] Water is inexpensive, nontoxic, and nonflammable. However, the major drawback of using it as a solvent in organic chemistry is the poor water solubility of organic compounds, which makes water incompatible with many synthetic methodologies. Although water presents some challenges when used as a solvent, it also provides the opportunity to provide safer and potentially more sustainable processes.[3] Therefore, researchers have worked to develop conditions under which a wide range of organic reactions can be conducted in aqueous reaction media.[4] However, aqueous-phase C−H functionalization reactions have received limited attention. Only a few recent research studies have shown that C−H functionalization can be performed in or on water and that water can allow the reactions to be performed under conditions milder than those in traditional organic solvents.[5] The direct arylation of electron-rich heteroaromatic compounds, including arylthiazoles, oxazoles, and indazoles, in water can be catalyzed with $Pd(dppf)Cl_2$ (dppf = 1,10-ferrocenebis(diphenylphosphine)) in the presence of Ag_2CO_3 with high yields.[6] Indoles can be arylated in the 2-position with aryl iodides using a catalyst derived from $Pd(OAc)_2$ and bis(diphenylphosphano)methane (5 mol %) at 110 °C in water.[7] Phosphine ligands, which are often toxic, air-sensitive, and expensive, are typically adopted.[8] The use of c-$C_6H_{11}CO_2Ag$ salts to promote direct arylations was proved to be successful, also employing an "on water" approach. Several 2-arylindoles were obtained in high yields by reacting the corresponding indoles with aryl iodides in neat water at 30 °C.[5b] Notably, the reaction did not work when free NH-indole was employed. Environmentally benign, operationally simple, and robust reactions, particularly those employing reusable solid catalysts, are of significant interest to the chemical industry.

Solid materials, which are prepared by generating and depositing or entrapping Pd particles onto or in solid supports, such as zeolite,[9] organic materials,[10] oxides,[11] carbonaceous materials,[12] and metal−organic frameworks (MOFs),[13] have

Received: September 25, 2015
Revised: December 1, 2015

DOI: 10.1021/acscatal.5b02147
ACS Catal. 2016, 6, 1062−1074

been explored as solid catalysts for the direct functionalization of C−H bonds. A simple heterogeneously palladium catalyzed procedure for the selective C3 arylation of indoles was reported by Cusati and Djakovitch[9] using $[Pd(NH_3)_4]^{2+}$/NaY as catalyst and K_2CO_3 as the base, in dioxane at reflux. High conversions and moderate to good isolated yields can be achieved with free *N*-H-indole, 2-methylindole, or 2-phenylindole under rather mild reaction conditions. Attempts to transpose this methodology to the selective arylation in pure water failed because the catalyst support dissolved under the reaction conditions. Glorius and co-workers have pioneered a heterogeneous version of the $C(sp^3)$−H α-arylation of ketones with magnetite-supported Pd NPs that are modified by chiral N-heterocyclic carbenes.[14] The chiral N-heterocyclic carbenes have a dominating effect on the catalytic activity and the level of enantioselection and allow for a heterogeneous mechanism. Subsequently, the same researchers adopted a ligand-free, dual catalytic system of heterogeneous Pd/C and CuCl for the complete and selective C3−H arylation of benzo[*b*]thiophenes with aryl chlorides.[15] Backvall, Olloffson, and co-workers have recently synthesized a heterogeneous catalyst based on Pd NPs that are supported on amino-functionalized mesocellular foam (Pd0-AmP-MCF) for the highly selective C2 arylation of indoles using diaryliodonium salts in water under mild conditions.[16] By comparison, commercial Pd/C shows negligible activity during this reaction.[16b] The high catalytic activity is attributed to the 2−3 nm Pd NPs and the three-dimensional network of mesoporous materials. However, the catalyst undergoes a continuous activity loss when it is recycled. Cao and co-workers reported that Pd NPs@MIL-101(Cr) was reusable for the C−H arylation of indoles with aryl iodides for at least five runs without significant deactivation.[13] The confinement of the Pd NPs inside the mesoporous cages of the MOFs (MIL-101(Cr)) and the interaction between Pd and the ionic framework may prevent strong leaching and particle growth. However, the reaction involved organic solvents, such as dimethylacetamide (DMA), *N*-methyl-2-pyrrolidone (NMP), or additives (Cs_2CO_3). Pd NPs on modified fluorous silica gel were also found to exhibit high performance in the C2 arylation of indoles with aryl iodides in the presence of DMA and CsOAc.[11b] Despite the negligible Pd leaching during the reaction, as observed from hot-filtration experiments, a reduction in the yield after six runs was detected. This observation did not completely refute the homogeneous contribution, because a rapid redeposition of the leached Pd species onto the support can occur under the reaction conditions,[12e,17] which has been widely reported in the Heck and Suzuki coupling reactions.[18]

While investigating the reactivity of solid catalysts in aqueous solution, we established an operationally simple C2 arylation of *N*-methylindole with diphenyliodonium salts. The synthesis of these Pd NPs supported on ordered mesoporous hybrid polymer-based materials that are modified with nitrogen-containing groups (Pd/ODDMA-MP) involves the micelle-templated approach. Ordered mesoporous materials have recently found widespread applications as catalyst supports because of their nanometer-sized porosity, which facilitates molecular diffusion, and their versatile surface functionalization, which allows the dispersion of metals.[19] In particular, the adsorption of reactants on hydrophobic carbonaceous supports in comparison to silicates is further promoted by van der Waals interactions, resulting in favorable reactant/product mass transport.[20] The arylation of *N*-methylindole over Pd/11.5ODDMA-MP is insensitive to air and moisture. Furthermore, hot filtration and mercapto-functionalized silica poison tests provide evidence of the negligible Pd leaching in the liquid phase. The catalysts can be reused a minimum of eight times without notable activity loss, particle aggregation, or structural destruction. Additional activation treatment is also avoided. The grafted long-chain quaternary ammonium functional groups play at least three vital roles in catalysis: (i) the coordination of Pd with an electron-rich environment, (ii) the dispersion and stabilization of Pd NPs that have a size of approximately 1.5 nm, and (iii) the facilitation of the diffusion of the aqueous organic reactant inside mesopores, which are sufficiently large to access active centers.

2. EXPERIMENTAL SECTION

2.1. Chemicals. Octadecyldimethyl[3-(trimethoxysilyl)-propyl]ammonium chloride (ODDMA, 60% in methanol), Na_2PdCl_4 (98%), $PdCl_2$ (98%), $Pd(OAc)_2$ (99%), $Pd(PPh_3)_4$ (99%), and 5% Pd/C (wetted with ca. 55% water) were purchased from Meryer Chemical Technology Co. Triblock copolymer PluronicP123 (poly(propylene oxide)-*block*-poly(ethylene oxide)-*block*-poly(propylene oxide), $PEO_{20}PPO_{70}PEO_{20}$, 5800) and PluronicF127 ($PEO_{106}PPO_{70}PEO_{106}$, 12600) were purchased from Aldrich Chemical Co. Mercapto-functionalized silica (SH-SiO_2, S loading 1.6 mmol/g) and diphenyliodonium triflate (98%) were purchased from J&K Chemical Co. Bis(4-methylphenyl)-iodonium triflate was synthesized according to the procedure of Olofssonet al. (see the Supporting Information).[21] The remaining chemicals were obtained from the Shanghai Chemical Company. All chemicals were used as received without further purification. The water used in all experiments was deionized.

2.2. Catalyst Preparation. The ordered mesoporous resin based supports were synthesized via a surfactant-templating method. The typical synthesis is as follows: 1.652 g of octadecyldimethyl[3-(trimethoxysilyl)propyl]ammonium chloride (ODDMA), 3.744 g of tetraethyl orthosilicate (TEOS), and 5.0 g of ethanol were mixed at 40 °C with stirring. A solution containing 2.4 g of triblock copolymer P123, 2.0 g of 0.2 M HCl, 10.0 g of ethanol, and 10.0 g of low-polymerized phenolic resin ethanolic solution (20 wt %, containing 1.22 g of phenol and 0.78 g of formaldehyde), which was prepared via the base-catalyzed polymerization of phenol and formaldehyde,[22] was added to this mixture in sequence. The mixture was then stirred for another 2 h. Then, the solution was poured into several dishes. After ethanol evaporation at room temperature for 8 h and thermopolymerization at 100 °C for 24 h, the films were scratched from the dishes. The as-made samples were then heated to 275 °C for 5 h under high-purity nitrogen to obtain ODDMA-functionalized mesoporous polymer-based materials. The concentration of the ODDMA was tuned by adjusting the ratio of ODDMA to TEOS while keeping the total molar content of SiO_2 constant. The final products are denoted as *n*ODDMA-MP, where *n* represents the percent mass content of the ODDMA functional groups, as estimated by elemental analysis. For a special purpose, the *n*ODDMA-MP sample was carbonized at 900 °C for 3 h to obtain a carbon-based composite, *n*ODDMA-MC. Subsequently, *n*ODDMA-MC was mixed with 45 mL of 1 M NaOH solution four times to remove the silica component (*n*ODDMA-MC-R).

Pristine mesoporous polymer based material (MP), silica (SBA-15), and mesoporous carbon (FDU-15) were also

DOI: 10.1021/acscatal.5b02147
ACS Catal. 2016, 6, 1062−1074

prepared according to the established procedures (see the Supporting Information).[23] A nonporous material (ODDMA-P) was synthesized in the absence of triblock copolymer P123, and the other chemicals and procedures were identical with those for 11.5ODDMA-MP.

The supported Pd catalysts were prepared using the ion-exchange method. In the typical procedure, 4.0 mL of an aqueous solution of Na_2PdCl_4 (2.5 wt %) was mixed with 0.3 g of dry 11.5ODDMA-MP carrier for 12 h with stirring. The mixture was filtered, washed with deionized water to remove the free Pd ions, and placed in a hood overnight. The solutions were collected to determine the Pd concentration using inductively coupled plasma-atomic emission spectrometry (ICP-AES, Varian VISTA-MPX). The catalysts were then dried at 50 °C under vacuum, reduced at 200 °C in a forming gas (10 vol % H_2 in nitrogen) for 3 h, and denoted as the fresh supported catalysts (Pd/11.5ODDMA-MP). The ICP-AES technique was applied to determine the Pd content in the solid. Both analyses confirmed that the Pd content was approximately 1 wt %. Pristine mesoporous polymer, silica, and mesoporous carbon supported Pd catalysts were prepared using the impregnation method according to the literature (Supporting Information).[19a]

2.3. Characterization. For the hot-filtration test, after 0.5 h-stirring of the setup experiment, the liquid phase was collected via hot filtration, added with 0.2 mmol of *N*-methylindole and further stirred for 4 h or 6 h. Then the aqueous mother liquor was extracted with toluene and analyzed. The separated solid was washed with water (2.5 mL), extracted twice with toluene (5.0 mL). The extraction was also analyzed. Powder X-ray diffraction (XRD) data were collected on a Rigaku Dmax-3C diffractometer equipped with Cu Kα radiation (40 kV, 30 mA, λ = 0.15408 nm). The formula $d = \lambda/2 \sin\theta$ was used to calculate the *d*-spacing values, and the formula $a_0 = 2d_{10}/\sqrt{3}$ was used to calculate the unit cell parameters. The metallic Pd sizes were calculated according to the Scherrer formula, size = $0.89\lambda/\beta \cos\theta$, on the basis of the (111) diffraction peak in the wide-angle XRD patterns. Gas adsorption experiments were performed using a Micromeritics TriStar II 3020 instrument. Nitrogen gas was used as the analysis adsorptive, and the isotherms were measured at cryogenic temperature (77.4 K). Brunauer–Emmett–Teller (BET) surface areas were calculated from the linear part of the adsorption isotherms (i.e., P/P_0 = 0.06–0.2). The pore volumes and pore size distributions were derived from the adsorption branches of the isotherms following the Barrett–Joyner–Halenda (BJH) model. The micropore volumes (V_{micro}) were calculated from the *V*–*t* plot method. The Pd/11.5ODDMA-MP and Pd/11.5ODDMA-MP-8 run samples were ultrasonically dispersed in ethanol, and then a drop of the solution was placed on a permeable C/Cu TEM grid for the TEM characterization. An FEI Tecnai G2 F20 microscope equipped with a HAADF-STEM detector that operates at 200 kV was used to perform the structural investigations in both TEM and STEM modes. The Fourier transform infrared (FT-IR) spectra were collected using a Nicolet Fourier spectrophotometer using KBr pellets of the solid samples. The C, H, N, and O contents were measured using a Vario EL III elemental analyzer (Germany). Thermogravimetric (TG) analysis curves were monitored using a Mettler Toledo 851e apparatus. The samples were heated from room temperature to 1000 °C at a rate of 10 °C/min under an air flow. X-ray photoelectron spectroscopy (XPS) analyses were performed on a PerkinElmer PHI 5000CESCA system with a base pressure of 10^{-9} Torr. The Pd loading on the carriers was determined using inductively coupled plasma-atomic emission spectrometry (ICP-AES, Varian VISTA-MPX). The ^{13}C and ^{29}Si solid-state nuclear magnetic resonance (NMR) experiments were performed on a Bruker DSX300 spectrometer (Germany). The ^{13}C CP-MAS NMR spectra were collected at room temperature with a frequency of 75 MHz (2 s of recycling, 2.5 ms of contact time) using adamantane as a reference under the conditions of cross-polarization (CP) and magic angle sample spinning (MAS). The ^{29}Si solid-state MAS NMR spectra were collected at room temperature with a frequency of 59.6 MHz, a recycling delay of 600 s, a radiation frequency intensity of 62.5 kHz, and a reference sample of Q_8M_8 ($[(CH_3)_3SiO]_8Si_8O_{12}$). The ζ potential vs pH curves were recorded using a ZEN 3600 instrument (Malvern Instruments). The ζ potential experiments were performed using a certain amount of 0.1 M NaOH and 0.1 M HCl to adjust the pH value of the specific sample water solution, including 0.1 M NaCl to maintain a high background electrolyte concentration. The H_2 chemisorption was conducted on a Micromeritics AutoChem II 2920 system by pulsing hydrogen on the supported Pd catalyst. The Pd surface areas were calculated from the H_2 chemisorption data, assuming that all Pd particles were spherical and that the adsorption stoichiometry was one H atom per Pd metal.[24]

2.4. Catalytic Reactions. The reactions were conducted in a 10 mL round-bottomed flask at 60 °C using water as the solvent. Typically, 25 μL (0.2 mmol) of *N*-methylindole and 0.172 g (0.4 mmol) of diphenyliodonium triflate (**2a**) were added to 2 mL of water and placed in the reactor. To this was added 0.021 g (containing 0.002 mmol of metallic Pd) of the supported Pd catalyst, and the mixture was heated to 60 °C. After 12 h of stirring, the products were hot filtered. The liquid phase was analyzed using ICP-AES to determine the leaching of Pd during the reaction; then, the liquid phase was extracted with toluene (5.0 mL) to analyze the conversion and selectivity. The solid was washed with water (2.5 mL) and toluene (5.0 mL), and the liquid phase was extracted with toluene and analyzed. The products were quantified using GC-mass analysis (Agilent 6890n equipped with a HP-5). The carbon balance was established with a 5% difference. The analysis was repeated for a minimum of three times for every test, and the experimental errors were within ±5%. The catalytic results are shown in terms of the absolute *N*-methyl-2-phenylindole yield, the initial reaction rate calculated at the beginning of the reaction ((mmol of reacted *N*-methylindole)/((mmol of Pd) h)), the turnover frequency (TOF, the rate based on the number of active sites, (initial rate)/(exposed surface atom ratio), and the turnover number (TON, (mmol of reacted *N*-methylindole)/((mmol of Pd)).[25] The products were also isolated and purified using column chromatography. The identification was conducted via ^1H NMR analysis on a Bruker DRX 400 spectrometer using tetramethylsilane as the internal standard.

An adsorption test was also performed. Approximately 0.4 mmol of diphenyliodonium triflate was dissolved in 2.0 mL of water and placed in the reactor. To this solution were added 0.021 g of the supported Pd catalyst and 0.2 mmol of *N*-methylindole at room temperature. After 2 h of stirring, the solid was separated, washed with water (2.5 mL), and extracted twice with toluene (5.0 mL). The aqueous mother liquor was also extracted with toluene. Both extracted liquid phases were analyzed via GC analysis.

DOI: 10.1021/acscatal.5b02147
ACS Catal. 2016, 6, 1062–1074

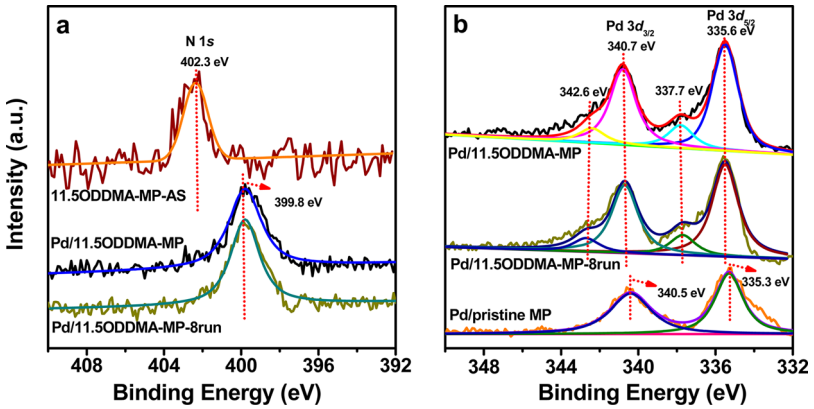

Figure 1. (a) N 1s XPS spectrum and (b) Pd 3d XPS spectra for the as-synthesized mesoporous 11.5ODDMA-MP and fresh and recycled supported Pd catalysts (Pd/pristine MP, Pd/11.5ODDMA-MP, and Pd/11.5ODDMA-MP-8run).

Table 1. Structural and Textural Properties for the Nitrogen-Containing Functional Group Modified Mesoporous Polymeric Carriers and Supported Pd Catalysts

sample	N content (wt %)	Pd content (wt %)	S_{BET} (m^2/g)	V_t (cm^3/g)	D_p (nm)	d_{Pd}[a] (nm)	d_{Pd}[b] (nm)
8.5ODDMA-MP	0.37	0	376	0.43	5.0		
11.5ODDMA-MP	0.5	0	343	0.44	5.0		
13ODDMA-MP	0.6	0	237	0.27	4.5		
pristine MP	0	0	324	0.52	8.0		
Pd/11.5ODDMA-MP	0.5	0.96	309	0.41	5.0	1.5	1.4
Pd/11.5ODDMA-MP-8run[c]	0.5	0.96	260	0.32	4.8	nd	1.8
Pd/pristine MP	0	0.95	320	0.52	8.0	4.0	3.4
Pd/FDU-15	0	0.98	1108	0.34	3.2	2.1	np[d]
Pd/SBA-15	0	0.98	852	1.2	9.0	10.6	8.2

[a]Particle size, calculated from the H_2 chemisorption. [b]Particle size, estimated from the TEM images. [c]Pd/11.5ODDMA-MP catalyst after eight catalytic runs. [d]np: not provided.

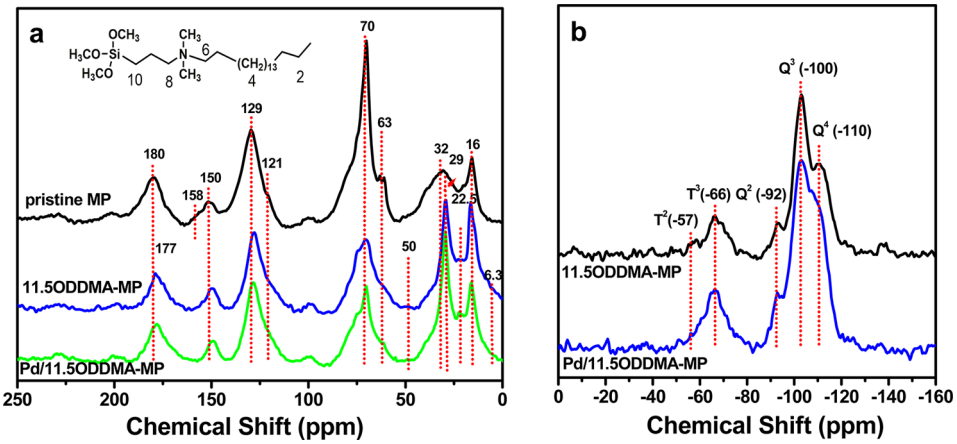

Figure 2. (a) ^{13}C CP-MAS NMR and (b) ^{29}Si MAS NMR spectra for the pristine MP, 11.5ODDMA-MP carrier, and Pd/11.5ODDMA-MP catalyst.

Mercapto-functionalized silica (SH-silica) was used as a trapping agent for the poisoning experiment.[26] Before the addition of the reaction solution, 0.044 g of SH-silica was typically added to the reaction flask with the molar ratio SH:Pd = 35:1.

For the reuse studies, the Pd/11.5ODDMA-MP catalyst was washed twice with toluene and subsequently with purified water after hot filtration. The catalyst was dried under vacuum at 100 °C overnight, weighed, and then reused. Parallel reactions were performed to ensure that the catalyst loading was identical in each run. After eight runs, the catalyst was characterized and denoted as Pd/11.5ODDMA-MP-8run.

3. RESULTS AND DISCUSSION

3.1. Synthesis of the Mesoporous Polymer. The N 1s peak, with a binding energy of approximately 402.3 eV, was detected in the XPS spectrum of the as-synthesized 11.5ODDMA-MP and corresponds to the nitrogen in a quaternary ammonium group (Figure 1a).[27] The TG curve for this sample shows a distinct weight loss beginning at 220 °C (the weight loss below 140 °C is related to the desorption of H_2O and the organic solvent; Figure S1 in the Supporting Information). Only 8 wt % of the organic substances including triblock copolymer P123, low-polymerized resin, and a functionalized alkyl quaternary ammonium group can be

DOI: 10.1021/acscatal.5b02147
ACS Catal. 2016, 6, 1062−1074

released at a temperature of 300 °C, and approximately 70 wt % of the substances can be removed up to 600 °C. For the present mesoporous material, nitrogen was adopted as the protecting gas, which can reduce the oxidation of both functional groups and phenolic resins, and therefore, the preservation of the quaternary ammonium salt upon heating to 275 °C is expected. The elemental analysis indicates nitrogen contents of 0.264, 0.357, and 0.404 mmol/g and 8.5, 11.5, and 13.0 wt % ODDMA for 8.5ODDMA-MP, 11.5ODDMA-MP, and 13ODDMA-MP, respectively (Table 1), demonstrating an increasing N content with the increase in the ODDMA functional group in the synthesis batch.

The solid-state ^{13}C CP-MAS NMR spectra of the pristine MP, 8.5ODDMA-MP, and Pd/11.5ODDMA-MP are shown in Figure 2a. The strong and broad resonance signals at approximately 129 and 150 ppm in the MP can be ascribed to the OH-substituted carbon in the phenol and to other aromatic carbons (except for the OH-substituted aromatic carbon), respectively.[28] The shoulder peaks at 121 ppm can be assigned to nonsubstituted aromatic ortho carbons, and the peak at 63 ppm can be assigned to hydroxymethyl groups at the ortho or para positions. The broad overlapping signals at approximately 32 ppm can be ascribed to methylene linkages between the phenolic rings. These results are similar to those for the mesoporous polymer (FDU-15-350),[23] indicating a polymer-based framework. An intense and narrow peak at 70 ppm that corresponds to the carbons in triblock copolymer P123[29] is also observed, implying the involvement of the template. The BET surface areas for the pristine MP are ordered as follows: before calcination (0) < calcination at 275 °C (324 m^2/g) < calcination at 350 °C (559 m^2/g). Because the triblock copolymer can be completely eliminated at a temperature of 350 °C,[30] the reduction in the BET surface area for the sample heated to 275 °C under nitrogen suggests the incomplete removal of the triblock copolymer. Partial pores are occupied by the triblock copolymer, in accordance with the NMR spectrum. The above resonance signals are also found in 11.5ODDMA-MP. The major difference is the appearance or enhancement of the signals between 50 and 20 ppm. The strongest resonance at 29 ppm indicates high populations of the trans or gauche-trans conformation in the alkyl chains (C4) of ODDMA. The peak at 22.5 ppm can be assigned to C2, C6 and C8, and the peak at approximately 50 ppm originates from the carbon in the methyl attached to nitrogen (C7). Finally, the peak at 6.3 ppm in the high-field can be attributed to the carbon connected to the Si atom (C10).[31] These results indicate the incorporation of the functional group ODDMA, in the hybrid solid. Two characteristic T^m signals, which are assigned to the Si species covalently bonded to the carbon atoms ($R\text{-}Si(OSi)_m(OH)_{3-m}$, the T^2 signal is weak) and three Q^n ($Si(OSi)_n(OH)_{4-n}$) silicons, are observed in the ^{29}Si MAS NMR spectrum of 11.5ODDMA-MP (Figure 2b), confirming the presence of bonds between the organic moieties and silica. The functionalization of the mesoporous polymer based materials was further investigated with FT-IR (Figure S2 in the Supporting Information). The pristine MP exhibits several bands at 3480, 1640, 1490, 1205, and 1067 cm^{-1}, which are assigned to the characteristic stretching modes of phenolic resins, the Si−O−Si vibration of silicate, and the C−O stretching of triblock copolymer F127. The improvement in the intensity of the absorption peaks of the C−H bonds (3000−2800 cm^{-1}) provides evidence of the presence of an octadecyl chain in ODDMA.[32] The weak adsorption peak at 1490 cm^{-1} corresponds to the C−N vibration and is overlapped with the vibrations in MP.

ζ potential measurements show that the isoelectric point (IEP) of the pristine MP is approximately 3.3, demonstrating that the surface has an overall negative charge at pH values above 3.3 (Figure 3).[33] The IEP value shifts toward higher pH

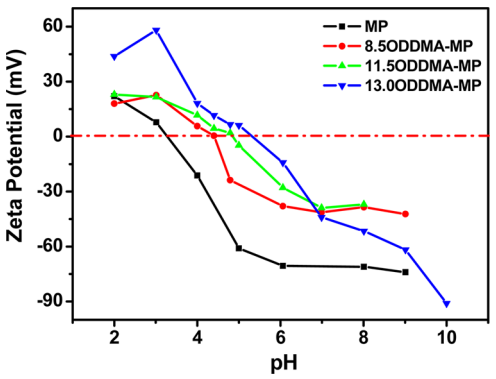

Figure 3. ζ potential for the pristine MP and ODDMA-MP materials with different functional group contents.

values of approximately 4.5 in the presence of the nitrogen-containing functional group (8.5ODDMA-MP) due to the inherent electropositive nature of quaternary ammonium salts.[34] With a further increase in nitrogen content, the samples exhibit increased IEP values of 4.8 and 5.3 for 11.5ODDMA-MP and 13ODDMA-MP, respectively. These results further demonstrate the immobilization of the nitrogen-containing functional group in mesoporous polymer based materials.

TEM images of 11.5ODDMA-MP exhibit well-arranged pores, confirming the ordered mesostructure (Figure S3 in the Supporting Information). The ordered mesostructure is observed in the large domains without a distinct defect. The ODDMA-functionalized mesoporous polymer materials display typical type IV nitrogen sorption isotherms with a sharp capillary condensation step at middle relative pressures, which is characteristic of mesoporous solids with uniform pore sizes (Figure 4). Asymmetrical hysteresis loops with shapes corresponding to the H2 type are observed.[35] Desorption branches are delayed to relative pressures near the fluid cavitation pressure.[36] Narrow pore-size distribution curves with a mean value of approximately 5.0 nm were calculated from the adsorption branches on the basis of the BJH model for functional polymer-based materials. This value is considerably smaller than that of the pristine polymer based materials (~8.0 nm), which may be due to the involvement of the long carbon chains of ODDMA in the mesopores. This is a common phenomenon for organic-functionalized mesoporous materials.[37] The BET surface area is between 237 and 376 m^2/g, and the pore volume is between 0.27 and 0.44 cm^3/g, similar to the case for pristine MP (Table 1).

One issue here is the integration of the functional group with the resin matrix. The pristine mesoporous polymer based material has been shown to possess an interpenetrated silicate and polymer framework in which resins and inorganic silica are well dispersed inside the pore walls.[30] After carbonization at 900 °C, each component can be removed individually. Both silica and carbon have an ordered mesostructure. Therefore, we carbonized the 8.5ODDMA-MP sample in nitrogen. Silica and carbon can be preserved at 900 °C, whereas the functional groups decompose. This sample exhibits a uniform pore size of

DOI: 10.1021/acscatal.5b02147
ACS Catal. 2016, 6, 1062−1074

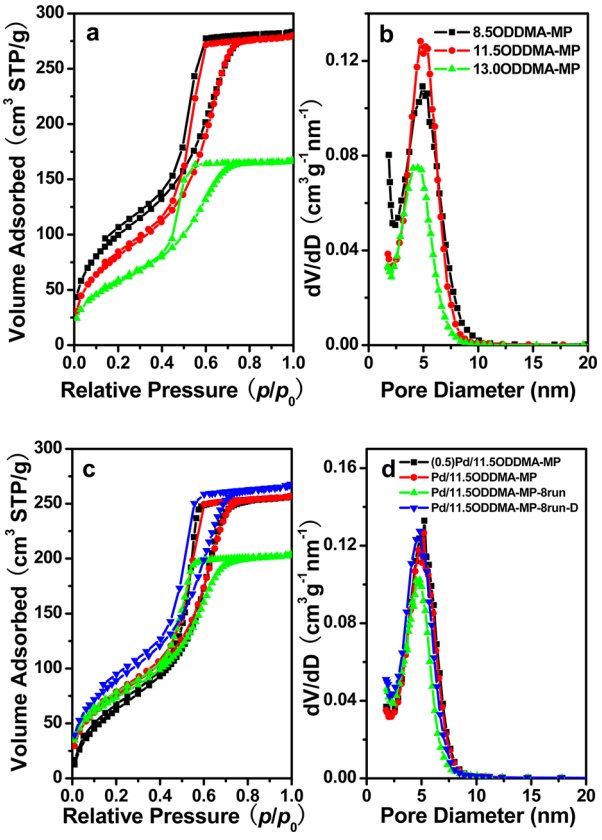

Figure 4. (a, c) N_2 sorption isotherms and (b, d) pore-size distribution curves of the ODDMA-functionalized organic−inorganic composites with different nitrogen contents and supported Pd catalysts. (0.5)Pd/11.5ODDMA-MP is a catalyst with 0.45 wt % Pd content. Pd/11.5ODDMA-MP-8run is a recycled catalyst after eight catalytic runs. Pd/11.5ODDMA-MP-8run-D is a recycled catalyst after heating to 200 °C under a N_2 flow.

3.4 nm, a BET surface area of 379 m^2/g, and a pore volume of 0.3 cm^3/g (Figure S4 in the Supporting Information), which are analogous to the values for carbonized pristine MP.[30] Further etching of silica leads to a sudden nitrogen adsorption at low relative pressures, corresponding to a dramatic increase in the BET surface area to 759 m^2/g and in the pore volume to 0.46 cm^3/g. The primary mesopore size is retained, and the contribution of the micropores to the adsorption amount is as low as 0.08 cm^3/g. Thus, small mesopores (approximately 1.8 nm) contribute primarily to the increase in the BET surface area and pore volume, which originates from the removal of silica NPs from the carbon pore walls.[30,38] A sample was also synthesized in the absence of triblock copolymers. Upon calcination at 900 °C, this sample shows an undetectable BET surface area (Figure S4). The distinct nitrogen adsorption at low relative pressures can be observed after dissolving the silica. The pore volume is 0.09 cm^3/g, and the micropore volume is approximately 0.03 cm^3/g, implying the generation of small mesopores in the carbon framework due to the etching of the silica component. These results may exclude the phase separation of silica and resins. The ODDMA-MP materials have an interpenetrated framework of silica and resins, and the primary mesopores originate from the triblock copolymer, similar to the case for pristine mesoporous polymer-based materials. Thus, the ODDMA moieties, which are initially linked to silicate, are grafted onto the polymer-based matrix from the self-assembly synthesis (Scheme 1).

Scheme 1. Synthetic Procedure for the Pd/*n*ODDMA-MP Catalyst

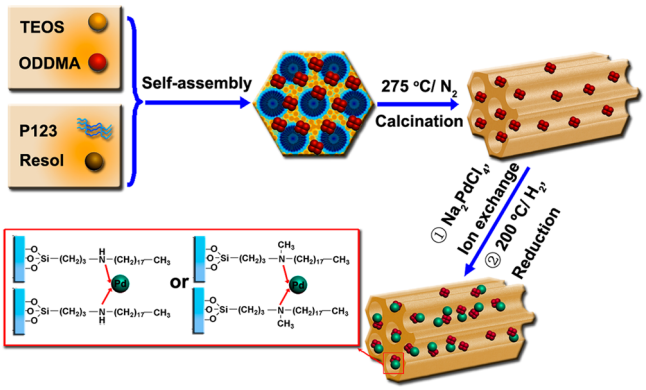

3.2. Dispersion of Metallic Pd in the Mesochannels.

After the incorporation of Pd into the ODDMA-modified MP matrix (0.96 wt %), the surface N:Pd molar ratio, which was estimated by the XPS analysis, is approximately 4.1 for Pd/11.5ODDMA-MP, in accordance with the elemental analysis. The Pd-containing catalyst displays solid-state ^{13}C CP-MAS and ^{29}Si MAS NMR spectra similar to those for the functionalized polymer carrier, implying the maintenance of the modified moieties after the incorporation of the Pd complex and the subsequent reduction to Pd NPs (Figure 2). The signal belonging to C7 cannot be clearly identified, implying the release of methyl groups. The XPS spectrum of the N 1s level for the fresh Pd/11.5ODDMA-MP catalyst exhibits a single signal at 399.8 eV (Figure 1a), which could be assigned for the NH bonds in amide[39] or quaternary nitrogen on Pd−N bond formation.[40] Paul and co-workers have investigated the decomposition of alkylammonium salts. The factors, including the number of long alkyl tails on the alkylammonium, exchanged metal ions, and the grafted inorganic clay in organoclays may play important roles in the degradation process. Methyl and benzyl groups in the organoclays were susceptible to nucleophilic attack by the halide anions via S_N2 nucleophilic substitution.[41] The grafted N can be therefore formed with release of CH_3Cl during reduction via nucleophilic substitution, in accordance with the NMR results (Scheme S1 in the Supporting Information).

The Pd 3d level indicates the presence of two chemically distinct spin−orbit pairs (Figure 1b). Each peak is broad, implying the possible presence of two overlapping peaks. A curve-fitting program was used to deconvolute the experimental data into two separate components. The major peaks were fit to 335.6 and 340.7 eV, which correspond to the Pd^0 $3d_{5/2}$ and $3d_{3/2}$ peaks, respectively,[42] but they are higher in energy in comparison with both Pd^0 in the literature and with pristine mesoporous polymer supported Pd (Pd/pristine MP).[43] The binding energies of the other component are 337.7 and 342.6 eV, which cannot be found in Pd/MP and are similar to an N-bound divalent Pd species.[39] A comparison of the areas under the $Pd^0{}_{5/2}$ and $Pd^{2+}{}_{5/2}$ peaks indicates that the relative ratio of Pd(0) to Pd(II) is approximately 5:1. Similar phenomena have been observed on Pd stabilized by chitosan with a signal of Pd(0), which is E_b(Pd $3d_{5/2}$) = 335.7 eV, in addition to Pd(II) (E_b(Pd $3d_{5/2}$) = 337.8 eV).[44] This corresponds to the reduction

DOI: 10.1021/acscatal.5b02147
ACS Catal. 2016, 6, 1062−1074

of metallic Pd accompanied by the coordination of Pd to the amide or quaternary N-containing groups in resins. However, a Pd−O coordination which comes from the benzyl or phenolic hydroxyl groups cannot be excluded. A left shift in the binding energy for both Pd(0) and Pd(II) has also been detected in Pd supported on carbon nanotubes that were functionalized with N-containing groups and mesoporous silicates.[45] Therefore, in the present catalyst, the N-containing group may stabilize the Pd atoms via coordination and thus create an electronically rich modification, similar to the case for the reduced Pd-chitosan complex (Scheme S1 in the Supporting Information).[44]

The Pd NPs were highly dispersed inside the well-arranged pores without any clear aggregation, as shown in the TEM images (Figure 5). The HAADF-STEM image (Figure 5b)

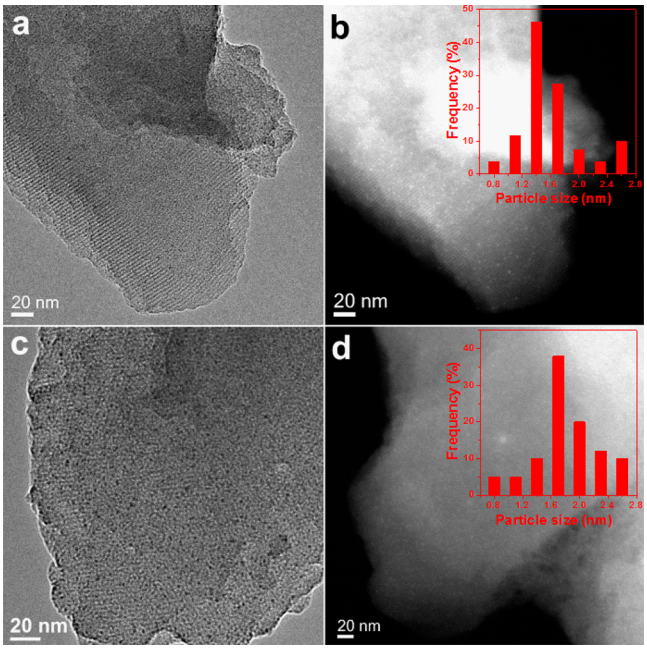

Figure 5. (a, c) TEM and (b, d) HAADF-STEM viewed perpendicular to the stripelike arranged pore patterns for (a, b) the fresh Pd/11.5ODDMA-MP and (c, d) the recycled Pd/11.5ODDMA-MP-8 run catalysts. The HAADF-STEM images were obtained for the same domain as or adjacent with TEM images. Insets in (b) and (d) are metal particle size distribution histograms.

clearly shows the dispersed small metal particles inside the mesochannels, and there is no visible aggregation outside the channels. The Pd particle size is approximately 1.4 nm. While we attempted to resolve the Pd crystalline structure, a relatively large Pd nanoparticle was chosen for the HRTEM investigation (Figure S5 in the Supporting Information). Pd nanoclusters with one part confined by the matrix and one part exposed can be clearly found, which can be further confirmed by the FFT pattern (Figure S5c). The indices of the crystal face are unresolved, possibly due to the small size or presence of amorphous Pd species. The size of the metallic Pd was determined to be 1.5 nm using H_2 chemisorption measurements, which is in good agreement with the TEM results. The wide-angle XRD patterns (Figure S6 in the Supporting Information) for the ODDMA-MP-supported Pd catalyst exhibit unresolved peaks, indicating the growth of relatively small Pd NPs, a low metallic content, or involvement of some amorphous Pd species.

The stable, well-distributed mesopore arrays were confirmed by type IV N_2 sorption isotherms (Figure 4). The pore-size distribution curve reflects the uniform size of the mesopores in the Pd catalysts, which are slightly smaller than their mother carriers. The BET surface area and pore volume are also slightly reduced after the incorporation of Pd, which is common for supported metal and metal oxide catalysts. The Pd content in the catalyst is tunable. A catalyst with 0.45 wt % Pd exhibits XRD patterns and N_2 sorption isotherms similar to those for a catalyst containing 0.96 wt %, suggesting the minor effect of the Pd content on the studied range of the Pd NP size and on the ordered mesostructure (Figure S6 in the Supporting Information, Figure 4, and Table 1).

We previously found that the growth of the Pd NPs is highly related to the interaction between the metallic solution and the internal pore wall of the mesoporous materials.[19a] For example, in the case of mesoporous silicate with a hydrophilic pore surface, the interaction between the silanol groups on the surface with the metallic solution favors the mass transfer of the Pd solution inside the mesochannels. Upon reduction, the metallic NPs aggregate together along the channels, and the sizes increase to approximately 9.0 nm (Figures S7−S10 in the Supporting Information). The mesoporous carbon FDU-15 possesses a hydrophobic and inert pore surface and many secondary micropores inside the pore walls. The diffusion of the metallic solution into the micropores due to the capillary force results in the formation of Pd NPs in the confined space or at the orifice of these micropores. No Pd NPs are observed in the TEM images (Figure S8). A mesoporous carbon−silica carrier with a synergistic role, which arises from the hybrid silica and carbonaceous nature of the framework together with the confinement of the mesochannel space, can yield a uniform dispersion of metallic Pd NPs with a size of approximately 3.4 nm.[19a] Similar Pd particles with a size of 3.4 nm can be formed inside the pristine MP mesopores, which is also likely due to the intrinsic hybrid pore channels. Metallic ions may be selectively adsorbed on the surface of silica, which can interact with the Pd ions, and the inert carbonaceous component may play a role in separating these ions. By comparison, the functionalization of the mesoporous polymer host by a nitrogen-containing functional group results in a charged pore surface. An acidified aqueous solution of $PdCl_4^{2-}$ anions can then be exchanged, and the ions are strongly adsorbed due to the strong interaction between the nitrogen-containing groups and the Pd species on the intrachannel surface.[32] After being decomposed and reduced by heating under a H_2 flow, the Pd complexes undergo metallic nucleation inside the mesoporous polymer based support.[46] The strong coordination between the N-containing group and Pd results in an electron-rich environment for the surface atoms, which can stabilize the nuclei and inhibit the transportation and aggregation of the NPs. Thus, NPs of approximately 1.5 nm in size can be achieved in the ODDMA-functionalized mesoporous polymers.

3.3. C2 Arylation of *N*-Methylindoles in Water. The ability to conduct direct C−H bond functionalization reactions under mild aqueous conditions is highly desirable. However, these reactions often require organic solvents, such as DMA,[10] DMF,[13] MeOH,[11d] DCM, and AcOH.[47] To our knowledge, only Backvall, Olloffson, and co-workers have reported the C2 arylation of indoles with diaryliodonium salts using Pd0-AmP-MCF (2.5 mol %) as a catalyst in water and under mild conditions.[16b] As noted above, a gradual decrease in the conversion from 100% to 80% and finally to 67% during the

DOI: 10.1021/acscatal.5b02147
ACS Catal. 2016, 6, 1062−1074

first three runs occurs, possibly because of the aggregation of the Pd NPs. In this case, the dissolution and redeposition of leaching Pd species onto solid catalysts during the reaction, which have been investigated in Pd-catalyzed coupling reactions, cannot be completely ruled out.[18]

The reactions reported here were conducted by using water as the solvent in batch reactors in air without any other additive at 60 °C (Figure 6). The mesoporous Pd/11.5ODDMA-MP

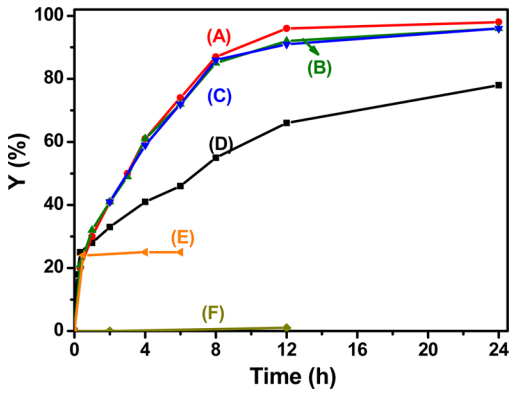

Figure 6. Plots of the *N*-methyl-2-phenylindole yield (reaction conditions: 0.002 mmol of Pd, 0.2 mmol of *N*-methylindole, and 0.4 mmol of Ph_2IOTf in water at 60 °C): (A) Pd/11.5ODDMA-MP activity without any poison; (B) Pd/11.5ODDMA-MP activity by adding SH-silica poison at the beginning of the reaction; (C) Pd/11.5ODDMA-MP activity by adding SH-silica after 2 h of reaction; (D) the control reaction using $Pd(OAc)_2$ as a catalyst without any poison; (E) the cessation of Pd/11.5ODDMA-MP activity by removing the catalyst via hot filtration after 0.5 h of reaction; (F) the cessation of $Pd(OAc)_2$ activity by adding SH-silica at the beginning of the reaction.

catalyst exhibits a TOF value of 82 h^{-1}, a high conversion (96%) of *N*-methyl-2-phenylindole, and selectivity (>99%) to *N*-methyl-2-phenylindole at 12 h (Table 2). Preliminary experiments performed using varying stirring speeds (in the range of 500−1000 rpm) indicated that the selected stirring

Table 2. Catalytic Performance of Different Catalysts in the Successive C−H Arylation of *N*-Methylindole[a]

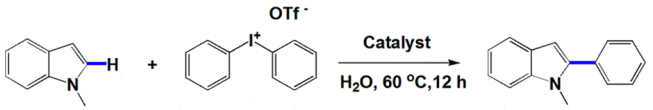

entry	catalyst	yield[b] (%)	*D*[c] (%)	TOF[d] (h^{-1})
1	Pd/11.5ODDMA-MP	96	73.4	82
2	Pd/pristine MP	81	28.2	24
3	Pd/SBA-15	72	10.7	62
4	Pd/FDU-15	55	53.8	9
5	Pd/C (commercial)	59	np[e]	np
6	$Pd(PPh_3)_4$	67		np
7	$Pd(OAc)_2$	66		np
8	$PdCl_2$	71		np
9[f]		0		np

[a]General reaction conditions: *N*-methylindole (0.2 mmol), Ph_2IOTf (0.4 mmol), H_2O (2.0 mL), reaction mixture stirred (800 rpm) at 60 °C in air for 12 h. [b]Determined by GC. [c]Palladium dispersion, calculated from the H_2 chemisorption. [d]TOF = (initial rate)/*D*, initial rate calculated at the beginning of the reaction (when the conversion reached ~20%). [e]np: not provided. [f]Without catalyst.

speed (800 rpm) enabled the reaction to proceed in the absence of diffusion limits under the present reaction conditions. To ensure a kinetic regime, two catalysts with Pd loadings of 0.45 and 0.96 wt % with similar Pd dispersions were used for the Madon−Boudart test.[48] The two catalysts with different Pd loadings exhibited similar TOF values of 84 ± 2 h^{-1}, confirming the kinetic regime.

The reaction was almost completely C2 selective, which is in good agreement with that of Pd0-AmP-MCF, but the TON value for a single run of 96 is considerably higher than the latter. We further compared our results with the reported solid catalyst, which used an organic solvent, and the compiled results are displayed in Table S1 in the Supporting Information.[11b,d,12d,13,15,16b,47] The present Pd/11.5ODDMA-MP catalyst shows a higher TON value than Pd/C, SiO_2@Fe_3O_4-triazole-Pd in the organic solvents.[11d,12d] However, it should be mentioned that the required iodonium salts may limit the application of the method in industry.

C−H functionalization reactions catalyzed by homogeneous palladium catalysts have been extensively studied.[1a] The homogeneous mechanistic pathways for the arylation of heteroaryl rings such as benzo[*b*]thiophenes as substrate have been summarized as follows (Scheme S2 in the Supporting Information): (i) direct C−H activation/palladation at C3 to give **1** followed by reductive elimination, (ii) palladation at C2 generating cationic species **2**, followed by aryl migration and elimination of Pd, (iii) a Heck-type mechanism with a requirement for syn *β*-hydride elimination and thus C−C bond rotation of cyclic intermediate **3**, and (iv) electrophilic palladation at C3 to give **4**, followed by reductive elimination and rearomatization.[15,49] However, the authors proposed that these traditional mechanisms associated with homogeneous catalysis were not directly applicable in the heterogeneous instance on the basis of their observations. The supported nature of the catalyst may have a direct impact on the regioselectivity of the reaction. Accordingly, they proposed an electrophilic reaction pathway which includes activation of the iodonium salt over a heterogeneous Pd/C catalyst. Activation of the iodonium salt in this manner has extensive precedent.[50] An electrophilic substitution in the arylation of 2-methylindole or 2-phenylindole using bromobenzene as the arylating agent that occurs through the coordination of an Ar−Pd−X complex to an indole nucleus has also been suggested on a $[Pd(NH_3)_4]^{2+}$/NaY solid catalyst.[9] Therefore, we also tentatively propose the oxidation addition of Pd to the C−I bond in the iodonium salt is the first activation step. Because oxidative addition involves oxidation (removal of electrons) of the metal center, the addition to the metal center is easier for a more electron-rich metal. The electron-rich surface Pd atoms that are coordinated with N in Pd/11.5ODDMA-MP may promote this process. Second, the presence of ODDMA may also render the Pd catalyst more accessible to the reactant. The enrichment of the reactant over Pd/11.5ODDMA-MP may accelerate the reaction and enable a high product yield. Further studies relating to the mechanism of the reaction and the role of the diaryliodonium salt are ongoing in our laboratory.

For the adsorption test in which the substrates and solid catalysts were mixed in water, trace substrates were detected in the aqueous solution upon extraction with toluene. However, the extracted solid catalyst consisted of 0.194 mmol of *N*-methylindole (97%). The carbon balance was calculated to be approximately 98%. These phenomena demonstrated the adsorption of substrates inside the pores, possibly due to the

DOI: 10.1021/acscatal.5b02147
ACS Catal. 2016, 6, 1062−1074

Table 3. C−H Arylation of the Indoles and Other Heterocycles with Diaryliodonium Salts using Pd/11.5ODDMA-MP[a]

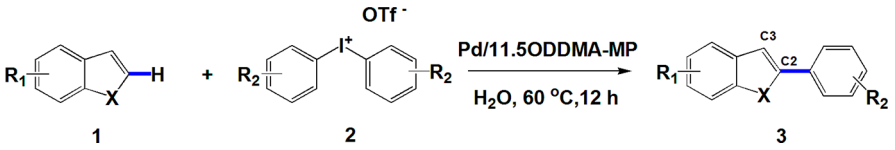

entry	X	R1	R2	yield (%)
1	NMe	H	p-CH_3	94 (**3b**)
2	NH	H	H	98 (**3c**)
3	NH	5-CH_3	H	96 (**3d**)
4	NH	7-Br	H	70 (**3e**)
5	NH	4-NO_2	H	29 (**3f**)
6	NH	5-OMe	H	56 (**3g**)
7[b]	O	H	H	90 (**3h**)
8[c]	S	H	H	89 (**3i**)

[a]General reaction conditions: indole (0.2 mmol), Ph_2IOTf (0.4 mmol), H_2O (2.0 mL), reaction mixture stirred (800 r/min) at 60 °C in air for 12 h. Yields refer to isolated products. C2:C3 > 99:1. [b]Benzo[*b*]furan (0.2 mmol). [c]Benzo[*b*]thiophene (0.2 mmol); C2:C3 < 1:99.

immobilization of the phase transfer agent, hydrophobic surface, and large mesopores in the catalyst. Moreover, the 74% yield of *N*-methyl-2-phenylindole and the 75% conversion of *N*-methylindole accounted for 98% of the carbon balance in the extracted liquid from the solid catalyst after 6 h of reaction and hot filtration. We confirmed both the enrichment of the substrates and the proceeding reaction inside the pores.[51]

After establishing the reaction conditions, we explored the symmetric diaryliodonium salt **2b** (Table 3). Bis(4-methylphenyl)iodonium triflate was successfully employed to give product **3b** in 94% yield. We subsequently explored the indole. Various substituted indoles were reacted to give the expected products in excellent yields (Table 3, **3c**−**g**). Both the N-protected indole and free *N*−H indole, which is considered to be less active than *N*-methylindole, were easily arylated in 98% (**3c**) and 96% (**3d**) yields, respectively. The synthesis of the bromo-substituted *N*−H indole **3e** was achieved with a high yield. The products are of particular interest because the bromide can function as a handle for further functionalization. However, only a few C-2 arylations of the Br-substituted substrate have been reported.[5b,52] The *N*−H indole derivative, which contains an electron-rich substituent of the benzene segment (**3g**), was obtained with a yield of 56%. The electron-withdrawing nitro group underwent a sluggish reaction (**3f**). Replacing the benzene ring of the *N*−H indole with a furan group produced the corresponding C2-arylated products with a 90% yield. Interestingly, the complete C3-selective arylation of benzo[*b*]thiophenes is obtained with a yield of 89%. Similar results have been found for a commercial Pd/C catalyst. However, a continuous decrease in yield was observed for the second (64%) and third (48%) cycles.[12d]

Several supported Pd catalysts were also further tested to convert *N*-methylindole via the C2 arylation reaction in water (the carriers are pristine MP, mesoporous carbon (FDU-15), silica (SBA-15), and commercial Pd/C (Table 2)). All catalysts exhibit >99% selectivity to the product. The yield of *N*-methyl-2-phenylindole within 12 h occurs in the following order: Pd/11.5ODDMA-MP > Pd/pristine MP > Pd/SBA-15 > Pd/C > Pd/FDU-15. However, the order for the TOF value is Pd/11.5ODDMA-MP > Pd/SBA-15 > Pd/pristine MP > Pd/FDU-15. The high activity for Pd/SBA-15 with a relatively large particle size is unusual. The difference will be discussed later.

3.4. Stability and Reusability of the Catalyst. Aside from the high conversion and TOF value, an important issue related to the solid catalyst is the reusability. The Pd leached in the liquid phase in the form of soluble colloids and molecular complexes may contribute to the activity but may reduce the reusability.[53]

The hot filtration test, in which solid catalysts are filtered out of the reaction and the filtrate is monitored for continued activity, has been considered a strong test for assessing the presence of soluble active Pd.[54] The reaction mixture was allowed to reach a 24% yield of *N*-methyl-2-phenylindole after 0.5 h of stirring before the liquid phase was collected via hot filtration (Figure 6E). The filtrate was kept at the reaction temperature with addition of 0.2 mmol of *N*-methylindole, and the conversion was monitored using GC. Negligible changes were observed in the yield of *N*-methyl-2-phenylindole after another 4 h of reaction time (<3%, less than the experimental error), which excludes the homogeneous catalysis in solution. The liquid phase of the reaction mixture that contained Pd/11.5ODDMA-MP was also collected via hot filtration after each reaction to test whether Pd leaches from the solid catalyst. The ICP-AES analysis confirms the presence of an undetectable amount of Pd in the reaction mixture (<0.05 ppm). However, the fact that the leached Pd rapidly forms inactive black Pd particles in the absence of stabilizers, which is often reported for homogeneous systems, cannot be excluded.[55] Furthermore, Pd species can dissolve in solution and then redeposit on the solid, as described above.[18c−e,56]

Mercapto-modified surfaces, such as SH-silica, have been used as effective Pd scavengers. They are rigid solids that do not swell under reaction conditions, a drawback of ligands that are immobilized on polymers such as poly(4-vinylpyridine). Thus, SH-silica was used as a selective poison to elucidate the type of catalysis (solution vs surface) that occurred with Pd, and we demonstrated its use as a more effective and versatile poison compared with poly(4-vinylpyridine) and Quadrapure TU.[57]

Bare, Pd-free SH-solid was used to "poison" the C2 arylation of *N*-methylindole with **2a** that was catalyzed by Pd/11.5ODDMA-MP or soluble molecular Pd. The S:Pd ratio was estimated to be 35:1. This sulfur ratio can sufficiently and rapidly capture soluble Pd species by overcoordination with neighboring mercapto groups before the leached Pd can be released back into solution.[26] For example, Jones and co-workers found that catalysis by soluble Pd species for Suzuki and Mizoroki−Heck coupling reactions can be quenched by the

DOI: 10.1021/acscatal.5b02147
ACS Catal. 2016, 6, 1062−1074

addition of SH-SiO_2 either at the initial stage or during the reaction.[26] In our study, the homogeneous $Pd(OAc)_2$ catalyst exhibits an initial reaction rate (108 mmol (mmol of Pd)$^{-1}$ h^{-1}) and product yield (78%, Figure 6D), implying that the Pd species prefer to aggregate in solutions and exhibit a relatively low product yield in comparison with Pd/11.5ODDMA-MP. The complete quenching of the catalysis was caused by the SH-SiO_2 poison, demonstrating the successful capture of the soluble Pd species by the mercapto-modified solid (Figure 6F). The homogeneous catalysts of $Pd(PPh_3)_4$ and $PdCl_2$ exhibited product yields of 67% and 71%, respectively, and the reaction was similarly quenched by the presence of SH-silica (Figure 7).

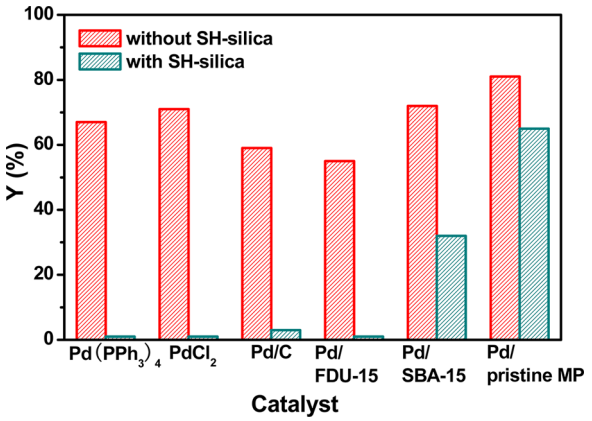

Figure 7. Comparison of the product yields for various catalysts in the absence or presence of the poisoning agent SH-silica for the C2 arylation of *N*-methylindole (reaction conditions: 0.002 mmol of Pd, 0.2 mmol of *N*-methylindole, 0.4 mmol of Ph_2IOTf, 2.0 mL of water, 60 °C, 12 h).

Commercial Pd/C was reported to proceed through a quasi-homogeneous mechanism with soluble Pd species that were leached from the support and redeposited onto charcoal, especially in C−C coupling reactions.[58] The commercial Pd/C can produce a yield of 59% product after 12 h. However, the product yield significantly decreases to 3% in the presence of the SH-silica poison (Figure 7). Similar results have been observed for Pd supported by mesoporous carbon (Pd/FDU-15). An almost entire quenching of the activity occurs with the presence of the trapping agent. Therefore, homogeneous soluble-catalyzed C−H bond functionalization is involved in this process, and both Pd/C and Pd/FDU-15 act as reservoirs for the Pd species in solution. The origin of commercial Pd/C is critical for its metal dispersion, surface functional groups, and surface areas. Thus, a detailed investigation of various commercial Pd/C should be conducted.

In comparison, the Pd/SBA-15 exhibits a 40% decrease in product yield in the presence of the trapping agent, implying that at least partial conversion is catalyzed by soluble Pd species. The pristine MP carrier possesses a distinct strong resistance to Pd leaching in comparison with silica SBA-15 and commercial carbon because the yield difference decreases by only 20% with SH-silica.

No difference in the kinetic profile of Pd/11.5ODDMA-MP was observed in the reactions with and without SH-silica (Figure 6B), confirming that the catalysis occurs inside the solid pores rather than in solution. When SH-silica was mixed with Pd/11.5ODDMA-MP after the reaction was initiated, an insignificant change in the original conversion was also observed (Figure 6C). These results clearly suggest that the contribution of soluble Pd species in the liquid phase to the performance of the catalyst is nearly entirely negligible. The strong coordination between the nitrogen-containing functional groups and Pd may stabilize the surface atoms and hence inhibit leaching into the solution. Thus, the reaction occurs over the Pd NPs inside the mesopores, which have high adsorption capacities for organic substances from water.[59] The enrichment of the substrate inside the pores and the enhancement of its accessibility to active Pd sites can improve the reaction to some extent.[56] Thus, the TOF values in Table 2 are not accurate due to the leaching of the Pd species of the solid catalysts during the reaction. However, an assumption that the Pd leaching is restricted inside the pores cannot be ruled out. The organic substrates are in a highly concentrated phase in water (not soluble) and that potential leaching or a molecular reaction would take place in this organic substrate phase. The dissolution and redeposition of leached Pd completely occur inside the pores, and after the reaction the catalyst can be entirely recovered. A thorough study combined with the following mechanistic investigation is deserving of further investigation.

For the recycling study, the C2 arylation of *N*-methylindole with **2a** was performed under the same reaction conditions as described above, except for the use of the recovered Pd/11.5ODDMA-MP catalyst. The reaction was repeated for 20 min (Figure 8a) because comparable yields may be obtained in successive reactions if an unnecessarily long time is selected for the first run, and 12 h was required to calculate the accumulative TON value (Figure 8b). Up to eight successive

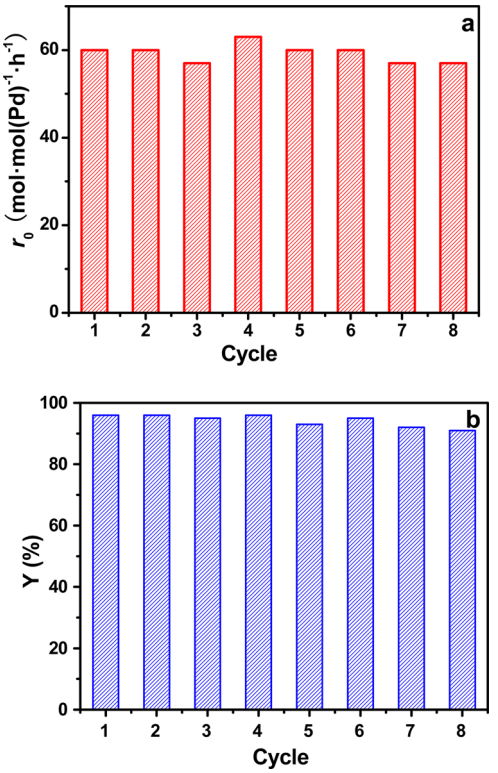

Figure 8. Compilation of the initial reaction rate (a) and product yield for the C2 arylation of *N*-methylindole in the successive runs with (b) the recovered Pd/11.5ODDMA-MP catalyst. In each run, the reaction conditions are 0.002 mmol of Pd, 0.2 mmol of *N*-methylindole, 0.4 mmol of Ph_2IOTf, 2 mL of water, 60 °C, 20 min (a) and 12 h (b).

DOI: 10.1021/acscatal.5b02147
ACS Catal. 2016, 6, 1062−1074

runs were tested. Both the initial reaction rate and product yield within 12 h for the recovered Pd/11.5ODDMA-MP (separated by hot filtration) were nearly the same for each run, indicating that the cumulative TON value for eight runs was 751. In contrast, the product yield for Pd/C reduces to 30% in the second run, respectively, similar to that found in the literature.[12d]

The tests on the collected successive mother liquors indicated an undetectable Pd content. The catalyst after eight runs was characterized using ICP-AES, XRD, TEM, and XPS techniques (Figures 1, 4, and 5 and Figure S6 in the Supporting Information). The results clearly show that the uniform pores of the long-range order, high-surface-area, and highly dispersed Pd NPs can be retained after several reactions. The Pd content, the surface N:Pd ratio, and Pd valence are similar to those of the fresh sample. These phenomena demonstrate that the solid catalyst is stable. N_2 sorption isotherms reflect a slight decrease in the sorption amounts and a decrease in the BET surface area and pore volume, which may be related to the accumulative organic substances inside the pores. We further heated the reused catalyst to 200 °C under a N_2 flow, and the BET surface area and pore volume were recovered (Figure 4). Therefore, the reaction conditions have a minor effect on the structure of the catalyst. The reusability of the Pd/11.5ODDMA-MP catalyst, which shows significant advantages over most reported solid catalysts, demonstrates its potential for industrial applications.

4. CONCLUSIONS

A nitrogen containing functional group modified and ordered mesoporous resin material, which was synthesized using the micelle-templated approach, was used to support a reusable solid Pd catalyst. The catalyst possesses an interpenetrated inorganic−organic framework. The grafted quaternary ammonium salt exhibits a negligible negative influence on the ordered mesopore arrays and pore blockage with a mass content of 11.5 wt %. Coordination with highly dispersed Pd NPs creates an electronically rich environment for surface atoms and causes a distinct enhancement in the stabilization and accessibility of these particles to organic substances in aqueous solution. The mesoporous Pd catalysts are active in the C2 arylation of *N*-methylindole with diphenyliodonium salt to yield *N*-methyl-2-phenylindole when water is used as the solvent without any other additive or the exclusion of air. The catalysis likely occurs on the Pd surface rather than in solution, as evidenced by a negligible reduction in activity upon the addition of mercapto-functionalized silica (SH-silica) poison but a significant quenching of the catalysis by the separation of solids via hot filtration. The heterogeneous mesoporous polymer based Pd catalysts are stable, exhibit undetected metal leaching, and can be reused more than eight times. The yields of target product for the Pd/SBA-15, Pd/pristine MP, commercial Pd/C, Pd/FDU-15, and even homogeneous catalysts ($Pd(OAc)_2$, $Pd(PPh_3)_4$, and $PdCl_2$) are lower than those on Pd/11.5ODDMA-MP, highlighting the important role of the integrated nitrogen-containing functional group on the pore wall on coordination with Pd.

■ ASSOCIATED CONTENT

Supporting Information

The Supporting Information is available free of charge on the ACS Publications website at DOI: 10.1021/acscatal.5b02147.

Preparation and characterization of low-polymerized phenolic resins, mesoporous carriers, and supported Pd catalysts, characterization of ODDMA-functionalized mesoporous polymer-based materials, including FT-IR spectra, TG curves, and TEM images, N_2 sorption isotherms and pore-size distribution curves for the control samples, XRD patterns of the fresh and used Pd catalysts with various contents, a comparison of the C−H arylation of the indoles (benzo[*b*]thiophene) catalyzed by different Pd catalysts, and the synthesis of diaryliodonium salts, 2-arylated indoles, and heterocycles (PDF)

■ AUTHOR INFORMATION

Corresponding Authors

*B.Z.: e-mail, bszhang@imr.ac.cn.

*Y.W.: tel, 86-21-6432-2516; fax, 86-21-6432-2511; e-mail, ywan@shnu.edu.cn.

Notes

The authors declare no competing financial interest.

■ ACKNOWLEDGMENTS

This work was supported by the State Key Basic Research Program of China (2013CB934102), the NSF of China (21322308 and 21173149), the Ministry of Education of China (PCSIRT-IRT1269 and 20123127110004), the International Joint Laboratory on Resource Chemistry (IJLRC), and the Shanghai Sci. & Tech. and Edu. Committee (11JC1409200, 14YF1409200, DZL123, and S30406). B.Z acknowledged the financial support by NSFC91545119 and Youth Innovation Promotion Association CAS (2015152).

■ REFERENCES

(1) (a) Lyons, T. W.; Sanford, M. S. *Chem. Rev.* **2010**, *110*, 1147−1169. (b) Cano, R.; Schmidt, A. F.; McGlacken, G. P. *Chem. Sci.* **2015**, *6*, 5338−5346. (c) Joucla, L.; Djakovitch, L. *Adv. Synth. Catal.* **2009**, *351*, 673−714. (d) Cacchi, S.; Fabrizi, G. *Chem. Rev.* **2011**, *111*, PR215−PR283.

(2) Molnár, Á. Catalyst Recycling in Palladium-Catalyzed Carbon-Carbon Coupling Reactions. In *Palladium-Catalyzed Coupling Reactions*. Molnár, Á., Ed.; Wiley-VCH: Weinheim, Germany, 2013; pp 333−386.

(3) (a) Butler, R. N.; Coyne, A. G. *Chem. Rev.* **2010**, *110*, 6302−6337. (b) Gawande, M. B.; Bonifacio, V. D. B.; Luque, R.; Branco, P. S.; Varma, R. S. *Chem. Soc. Rev.* **2013**, *42*, 5522−5551. (c) Zuo, Y.-J.; Qu, J. *J. Org. Chem.* **2014**, *79*, 6832−6839.

(4) (a) Li, C. J. *Chem. Rev.* **1993**, *93*, 2023−2035. (b) Herrerías, C. I.; Yao, X.; Li, Z.; Li, C.-J. *Chem. Rev.* **2007**, *107*, 2546−2562. (c) Li, B.; Dixneuf, P. H. *Chem. Soc. Rev.* **2013**, *42*, 5744−5767.

(5) (a) Wencel-Delord, J.; Dröge, T.; Liu, F.; Glorius, F. *Chem. Soc. Rev.* **2011**, *40*, 4740−4761. (b) Islam, S.; Larrosa, I. *Chem. - Eur. J.* **2013**, *19*, 15093−15096.

(6) (a) Ohnmacht, S.; Culshaw, A.; Greaney, M. *Org. Lett.* **2010**, *12*, 224−226. (b) Ohnmacht, S. A.; Mamone, P.; Culshaw, A. J.; Greaney, M. F. *Chem. Commun.* **2008**, 1241−1243. (c) Turner, G. L.; Morris, J. A.; Greaney, M. F. *Angew. Chem., Int. Ed.* **2007**, *46*, 7996−8000.

(7) Joucla, L.; Batail, N.; Djakovitch, L. *Adv. Synth. Catal.* **2010**, *352*, 2929−2936.

(8) (a) Fortman, G. C.; Nolan, S. P. *Chem. Soc. Rev.* **2011**, *40*, 5151−5169. (b) Bedford, R. B.; Cazin, C. S. J.; Holder, D. *Coord. Chem. Rev.* **2004**, *248*, 2283−2321. (c) Phan, N. T. S.; Van Der Sluys, M.; Jones, C. W. *Adv. Synth. Catal.* **2006**, *348*, 609−679. (d) Comanescu, C. C.; Iluc, V. M. *Inorg. Chem.* **2014**, *53*, 8517−8528.

(9) Cusati, G.; Djakovitch, L. *Tetrahedron Lett.* **2008**, *49*, 2499−2502.

DOI: 10.1021/acscatal.5b02147
ACS Catal. 2016, 6, 1062−1074

(10) Zinovyeva, V. A.; Vorotyntsev, M. A.; Bezverkhyy, I.; Chaumont, D.; Hierso, J.-C. *Adv. Funct. Mater.* **2011**, *21*, 1064−1075.
(11) (a) Chen, J.; He, L.; Natte, K.; Neumann, H.; Beller, M.; Wu, X. F. *Adv. Synth. Catal.* **2014**, *356*, 2955−2959. (b) Wang, L.; Yi, W.-b.; Cai, C. *Chem. Commun.* **2011**, *47*, 806−808. (c) Lee, J.; Chung, J.; Byun, S. M.; Kim, B. M.; Lee, C. *Tetrahedron* **2013**, *69*, 5660−5664. (d) Zhang, L.; Li, P.; Liu, C.; Yang, J.; Wang, M.; Wang, L. *Catal. Sci. Technol.* **2014**, *4*, 1979−1988.
(12) (a) Parisien, M.; Valette, D.; Fagnou, K. *J. Org. Chem.* **2005**, *70*, 7578−7584. (b) Jafarpour, F.; Rahiminejadan, S.; Hazrati, H. *J. Org. Chem.* **2010**, *75*, 3109−3112. (c) Tang, D.-T. D.; Collins, K. D.; Glorius, F. *J. Am. Chem. Soc.* **2013**, *135*, 7450−7453. (d) Tang, D. T. D.; Collins, K. D.; Ernst, J. B.; Glorius, F. *Angew. Chem., Int. Ed.* **2014**, *53*, 1809−1813. (e) Djakovitch, L.; Felpin, F.-X. *ChemCatChem* **2014**, *6*, 2175−2187.
(13) Huang, Y.; Lin, Z.; Cao, R. *Chem. - Eur. J.* **2011**, *17*, 12706−12712.
(14) Ranganath, K. V. S.; Kloesges, J.; Schäfer, A. H.; Glorius, F. *Angew. Chem., Int. Ed.* **2010**, *49*, 7786−7789.
(15) Tang, D.-T. D.; Collins, K. D.; Glorius, F. *J. Am. Chem. Soc.* **2013**, *135*, 7450−7453.
(16) (a) Johnston, E. V.; Verho, O.; Kärkäs, M. D.; Shakeri, M.; Tai, C.-W.; Palmgren, P.; Eriksson, K.; Oscarsson, S.; Bäckvall, J.-E. *Chem. - Eur. J.* **2012**, *18*, 12202−12206. (b) Malmgren, J.; Nagendiran, A.; Tai, C.-W.; Bäckvall, J.-E.; Olofsson, B. *Chem. - Eur. J.* **2014**, *20*, 13531−13535.
(17) (a) Djakovitch, L.; Rollet, P. *Tetrahedron Lett.* **2004**, *45*, 1367−1370. (b) Djakovitch, L.; Rollet, P. *Adv. Synth. Catal.* **2004**, *346*, 1782−1792. (c) Joucla, L.; Cusati, G.; Pinel, C.; Djakovitch, L. *Appl. Catal., A* **2009**, *360*, 145−153. (d) Rollet, P.; Kleist, W.; Dufaud, V.; Djakovitch, L. *J. Mol. Catal. A: Chem.* **2005**, *241*, 39−51.
(18) (a) Davies, I. W.; Matty, L.; Hughes, D. L.; Reider, P. J. *J. Am. Chem. Soc.* **2001**, *123*, 10139−10140. (b) Lipshutz, B. H.; Tasler, S.; Chrisman, W.; Spliethoff, B.; Tesche, B. *J. Org. Chem.* **2003**, *68*, 1177−1189. (c) MacQuarrie, S.; Horton, J. H.; Barnes, J.; McEleney, K.; Loock, H.-P.; Crudden, C. M. *Angew. Chem., Int. Ed.* **2008**, *47*, 3279−3282. (d) Köhler, K.; Heidenreich, R. G.; Soomro, S. S.; Pröckl, S. S. *Adv. Synth. Catal.* **2008**, *350*, 2930−2936. (e) Soomro, S. S.; Ansari, F. L.; Chatziapostolou, K.; Köhler, K. *J. Catal.* **2010**, *273*, 138−146.
(19) (a) Wan, Y.; Wang, H.; Zhao, Q.; Klingstedt, M.; Terasaki, O.; Zhao, D. *J. Am. Chem. Soc.* **2009**, *131*, 4541−4550. (b) Wang, S.; Zhao, Q.; Wei, H.; Wang, J.-Q.; Cho, M.; Cho, H. S.; Terasaki, O.; Wan, Y. *J. Am. Chem. Soc.* **2013**, *135*, 11849−11860. (c) Duan, L.; Fu, R.; Xiao, Z.; Zhao, Q.; Wang, J.-Q.; Chen, S.; Wan, Y. *ACS Catal.* **2015**, *5*, 575−586.
(20) (a) Zhuang, X.; Zhao, Q.; Wan, Y. *J. Mater. Chem.* **2010**, *20*, 4715−4724. (b) Wan, Y.; Zhang, D.; Zhai, Y.; Feng, C.; Chen, J.; Li, H. *Chem. - Asian J.* **2007**, *2*, 875−881.
(21) Bielawski, M.; Zhu, M.; Olofsson, B. *Adv. Synth. Catal.* **2007**, *349*, 2610−2618.
(22) Wan, Y.; Shi, Y.; Zhao, D. *Chem. Mater.* **2008**, *20*, 932−945.
(23) Meng, Y.; Gu, D.; Zhang, F.; Shi, Y.; Yang, H.; Li, Z.; Yu, C.; Tu, B.; Zhao, D. *Angew. Chem., Int. Ed.* **2005**, *44*, 7053−7059.
(24) Wang, S. Y.; Moon, S. H.; Vannice, M. A. *J. Catal.* **1981**, *71*, 167−174.
(25) (a) Della Pina, C.; Falletta, E.; Rossi, M.; Sacco, A. *J. Catal.* **2009**, *263*, 92−97. (b) Davis,M. E.; Davis, R. J. *Fundamentals of Chemical Reaction Engineering*; McGraw-Hill: New York, 2003; p 201.
(26) Richardson, J. M.; Jones, C. W. *J. Catal.* **2007**, *251*, 80−93.
(27) Gniewek, A.; Trzeciak, A. M.; Ziółkowski, J. J.; Kępiński, L.; Wrzyszcz, J.; Tylus, W. *J. Catal.* **2005**, *229*, 332−343.
(28) Grenier-Loustalot, M.-F.; Larroque, S.; Grenier, P. *Polymer* **1996**, *37*, 639−650.
(29) Yang, C.-M.; Zibrowius, B.; Schmidt, W.; Schüth, F. *Chem. Mater.* **2003**, *15*, 3739−3741.
(30) Liu, R.; Shi, Y.; Wan, Y.; Meng, Y.; Zhang, F.; Gu, D.; Chen, Z.; Tu, B.; Zhao, D. *J. Am. Chem. Soc.* **2006**, *128*, 11652−11662.
(31) (a) Ma, Y.; Xing, L.; Zheng, H.; Che, S. *Langmuir* **2011**, *27*, 517−520. (b) Fujii, K.; Hayashi, S.; Kodama, H. *Chem. Mater.* **2003**, *15*, 1189−1197.
(32) Yang, C. M.; Sheu, H. S.; Chao, K. J. *Adv. Funct. Mater.* **2002**, *12*, 143−148.
(33) Tomalia, D. A.; Naylor, A. M.; Goddard, W. A. *Angew. Chem., Int. Ed. Engl.* **1990**, *29*, 138−175.
(34) Teng, W.; Wu, Z.; Feng, D.; Fan, J.; Wang, J.; Wei, H.; Song, M.; Zhao, D. *Environ. Sci. Technol.* **2013**, *47*, 8633−8641.
(35) (a) Yu, C.; Chu, H.; Wan, Y.; Zhao, D. *J. Mater. Chem.* **2010**, *20*, 4705−4714. (b) Sing, K. S. *Pure Appl. Chem.* **1985**, *57*, 603−619.
(36) (a) Kleitz, F.; Czuryszkiewicz, T.; Solovyov, L. A.; Lindén, M. *Chem. Mater.* **2006**, *18*, 5070−5079. (b) Thommes, M.; Smarsly, B.; Groenewolt, M.; Ravikovitch, P. I.; Neimark, A. V. *Langmuir* **2006**, *22*, 756−764. (c) Groen, J. C.; Peffer, L. A. A.; Pérez-Ramírez, J. *Microporous Mesoporous Mater.* **2003**, *60*, 1−17.
(37) Hu, Q.; Hampsey, J. E.; Jiang, N.; Li, C.; Lu, Y. *Chem. Mater.* **2005**, *17*, 1561−1569.
(38) Wang, W.; Zhuang, X.; Zhao, Q.; Wan, Y. *J. Mater. Chem.* **2012**, *22*, 15874−15886.
(39) Arrigo, R.; Schuster, M. E.; Xie, Z.; Yi, Y.; Wowsnick, G.; Sun, L. L.; Hermann, K. E.; Friedrich, M.; Kast, P.; Hävecker, M. *ACS Catal.* **2015**, *5*, 2740−2753.
(40) (a) Wagner, A. J.; Wolfe, G. M.; Fairbrother, D. H. *Appl. Surf. Sci.* **2003**, *219*, 317−328. (b) Ozaki, J.-i.; Tanifuji, S.-i.; Furuichi, A.; Yabutsuka, K. *Electrochim. Acta* **2010**, *55*, 1864−1871.
(41) (a) Cui, L.; Khramov, D. M.; Bielawski, C. W.; Hunter, D. L.; Yoon, P. J.; Paul, D. R. *Polymer* **2008**, *49*, 3751−3761. (b) Xie, W.; Gao, Z.; Pan, W.-P.; Hunter, D.; Singh, A.; Vaia, R. *Chem. Mater.* **2001**, *13*, 2979−2990. (c) Cervantes-Uc, J. M.; Cauich-Rodríguez, J. V.; Vázquez-Torres, H.; Garfias-Mesías, L. F.; Paul, D. R. *Thermochim. Acta* **2007**, *457*, 92−102.
(42) (a) Militello, M. C.; Simko, S. J. *Surf. Sci. Spectra* **1994**, *3*, 387−394. (b) Huang, Y.; Gao, S.; Liu, T.; Lü, J.; Lin, X.; Li, H.; Cao, R. *ChemPlusChem* **2012**, *77*, 106−112. (c) Kovtunov, K. V.; Barskiy, D. A.; Salnikov, O. G.; Khudorozhkov, A. K.; Bukhtiyarov, V. I.; Prosvirin, I. P.; Koptyug, I. V. *Chem. Commun. (Cambridge, U. K.)* **2014**, *50*, 875−878. (d) Ji, Y.; Jain, S.; Davis, R. J. *J. Phys. Chem. B* **2005**, *109*, 17232−17238.
(43) Brun, M.; Berthet, A.; Bertolini, J. *J. Electron Spectrosc. Relat. Phenom.* **1999**, *104*, 55−60.
(44) Kramareva, N. V.; Stakheev, A. Y.; Tkachenko, O. P.; Klementiev, K. V.; Grünert, W.; Finashina, E. D.; Kustov, L. M. *J. Mol. Catal. A: Chem.* **2004**, *209*, 97−106.
(45) Zhang, Y.; He, X.; Ouyang, J.; Yang, H. *Sci. Rep.* **2013**, *3*, 2948.
(46) Yang, C.-m.; Liu, P.-h.; Ho, Y.-f.; Chiu, C.-y.; Chao, K.-j. *Chem. Mater.* **2003**, *15*, 275−280.
(47) Huang, Y.; Ma, T.; Huang, P.; Wu, D.; Lin, Z.; Cao, R. *ChemCatChem* **2013**, *5*, 1877−1883.
(48) Madon, R. J.; Boudart, M. *Ind. Eng. Chem. Fundam.* **1982**, *21*, 438−447.
(49) (a) Ueda, K.; Yanagisawa, S.; Yamaguchi, J.; Itami, K. *Angew. Chem., Int. Ed.* **2010**, *49*, 8946−8949. (b) Simmons, E. M.; Hartwig, J. F. *Angew. Chem., Int. Ed.* **2012**, *51*, 3066−3072. (c) De Meijere, A.; Meyer, F. E. *Angew. Chem., Int. Ed. Engl.* **1995**, *33*, 2379−2411. (d) Beletskaya, I. P.; Cheprakov, A. V. *Chem. Rev.* **2000**, *100*, 3009−3066. (e) Liégault, B. t.; Petrov, I.; Gorelsky, S. I.; Fagnou, K. *J. Org. Chem.* **2010**, *75*, 1047−1060.
(50) (a) Ochiai, M.; Shu, T.; Nagaoka, T.; Kitagawa, Y. *J. Org. Chem.* **1997**, *62*, 2130−2138. (b) Oh, C. H.; Kim, J. S.; Jung, H. H. *J. Org. Chem.* **1999**, *64*, 1338−1340. (c) Xiao, B.; Fu, Y.; Xu, J.; Gong, T.-J.; Dai, J.-J.; Yi, J.; Liu, L. *J. Am. Chem. Soc.* **2010**, *132*, 468−469. (d) Wang, B.; Graskemper, J. W.; Qin, L.; DiMagno, S. G. *Angew. Chem., Int. Ed.* **2010**, *49*, 4079−4083. (e) Ciana, C. L.; Phipps, R. J.; Brandt, J. R.; Meyer, F. M.; Gaunt, M. J. *Angew. Chem., Int. Ed.* **2011**, *50*, 458−462. (f) Allen, A. E.; MacMillan, D. W. *J. Am. Chem. Soc.* **2011**, *133*, 4260−4263. (g) Petersen, T. B.; Khan, R.; Olofsson, B. *Org. Lett.* **2011**, *13*, 3462−3465. (h) Neufeldt, S. R.; Sanford, M. S. *Adv. Synth. Catal.* **2012**, *354*, 3517−3522.

DOI: 10.1021/acscatal.5b02147
ACS Catal. 2016, 6, 1062−1074

(51) Liu, F.; Wang, L.; Sun, Q.; Zhu, L.; Meng, X.; Xiao, F.-S. *J. Am. Chem. Soc.* **2012**, *134*, 16948−16950.
(52) (a) Miao, T.; Li, P.; Wang, G. W.; Wang, L. *Chem. - Asian J.* **2013**, *8*, 3185−3190. (b) Deprez, N. R.; Kalyani, D.; Krause, A.; Sanford, M. S. *J. Am. Chem. Soc.* **2006**, *128*, 4972−4973. (c) Malmgren, J.; Nagendiran, A.; Tai, C. W.; Bäckvall, J. E.; Olofsson, B. *Chem. - Eur. J.* **2014**, *20*, 13531−13535.
(53) (a) Felpin, F. X.; Ayad, T.; Mitra, S. *Eur. J. Org. Chem.* **2006**, *2006*, 2679−2690. (b) Webb, J. D.; MacQuarrie, S.; McEleney, K.; Crudden, C. M. *J. Catal.* **2007**, *252*, 97−109.
(54) Sheldon, R. A.; Wallau, M.; Arends, I. W.; Schuchardt, U. *Acc. Chem. Res.* **1998**, *31*, 485−493.
(55) Balanta, A.; Godard, C.; Claver, C. *Chem. Soc. Rev.* **2011**, *40*, 4973−4985.
(56) Soomro, S. S.; Röhlich, C.; Köhler, K. *Adv. Synth. Catal.* **2011**, *353*, 767−775.
(57) Crudden, C. M.; Sateesh, M.; Lewis, R. *J. Am. Chem. Soc.* **2005**, *127*, 10045−10050.
(58) Nassar-Hardy, L.; Deraedt, C.; Fouquet, E.; Felpin, F. X. *Eur. J. Org. Chem.* **2011**, *2011*, 4616−4622.
(59) Zhuang, X.; Wan, Y.; Feng, C.; Shen, Y.; Zhao, D. *Chem. Mater.* **2009**, *21*, 706−716.

DOI: 10.1021/acscatal.5b02147
ACS Catal. 2016, 6, 1062−1074